Thermodynamic and Thermoeconomic investigation of an Integrated Gasification SOFC and Stirling Engine

Rokni, Masoud

Published in:
Proceedings of the 8th Conference on Sustainable Development of Energy, Water and Environment Systems

Publication date:
2013

SDEWES2013 Conference, Dubrovnik, Croatia, pp:0166-1 to 0166-23.

THERMODYNAMIC AND THERMOECONOMIC INVESTIGATION OF AN INTEGRATED GASIFICATION SOFC AND STIRLING ENGINE

Masoud Rokni
Department of Mechanical Engineering
Thermal Energy Section, Copenhagen, Denmark
e–mail: MR@mek.dtu.dk

ABSTRACT

Thermodynamic and thermoeconomic investigation of a small scale Integrated Gasification Solid Oxide Fuel Cell (SOFC) and Stirling engine for combined heat and power (CHP) with a net electric capacity of 120kW have been performed. Woodchips are used as gasification feedstock to produce syngas which is then utilized for feeding the anode side of SOFC stacks. Thermal efficiency of 0.424 LHV for the plant is found to use 89.4kg/h of feedstock for producing 120kW of electricity. Thermoeconomic analysis shows that the production price of electricity is 0.1204$/kWh. Further, hot water is considered as a by-product and the cost of hot water was found to be 0.0214$/kWh. When compared to other renewable systems at similar scale, it shows that if both SOFC and Stirling engine technology emerges enter commercialization phase, then they can deliver electricity at a cost rate which is competitive with corresponding renewable systems at the same size and therefore.

KEYWORDS

SOFC, Stirling, fuel cell, hybrid cycle, gasification, thermoeconomy.

INTRODUCTION

With an ever increasing demand for more efficient power production and distribution, the main research and development for the electricity production are identifies as efficiency enchantments and pollutant reduction, especially carbon dioxide among others. Today there is an increased interest of developing a distributed system of smaller scale facilities than large scale capacity at a specified location. It means that the electricity and heat can be produced and distributed close to the end user, and thereby minimize the costs associate with transportation [1, 2].

SOFC stacks will soon enter commercialization phase, while small Stirling engines has almost reached this phase. Therefore it might be interesting to combine these two technologies in a single system which would then quantify the benefits of each system to establish a new technology. Together, with an integrated gasification plant that gasifies wood chips in a two steps gasification process, one then may produce electricity and heat in an environmentally friendly way.

The SOFC is one of the most promising types of fuel cells, particularly when it comes to energy production. They are expected to produce clean electrical energy at high convention rates, with low noise and low emissions when it comes to pollution [3].

Due to high exhaust temperatures from SOFC caused by the high operating temperature of the cells and the fact that the fuel utilization in the fuel cell never reaches 100 %, the unreacted fuels needs to be combusted in burner which in turn produces off-gases with even higher temperature

that perfectly can be used in a heat engine, such as a Stirling engine, for production of power and heat for domestic purposes.
There exist numerous investigations on SOFC-based power systems suggesting high thermal efficiencies in the open literature. However, the majority of the studies use gas turbines as the bottoming cycle see e.g. [4, 5, 6]. Sometimes, a steam turbine (ST) was also used as a bottoming cycle [7] resulting in high plant efficiency. Only a few number of studies have been carried out with Stirling engine as a bottoming cycle when a fuel cell cycle is used as topping cycle, see e.g. [1]. At present using Brayton cycle and Rankine cycle as bottoming cycles seems to be more applicable, because of maturity of these technologies. As the development suggest that the operating temperature of the SOFC shall be decreased, then using gas turbine as bottoming cycle will be less beneficial.
Integrated gasification SOFC systems have also been studied for a while, see for example [8, 9, 10]. But there is no study on integrated biomass gasification SOFC-Stirling CHP plants in the open literature which is also the basis of this study.
The present work is an analytical study that conducts both thermodynamic and thermoeconomic investigation of systems with integrated gasification of wood chips, where the syngas is used as fuel for a SOFC plant which is also functioning as a topping cycle for a Stirling engine by utilizing the heat from the off-gasses exhausted from the topping cycle. System net capacity is 120kW which is suitable for decentralized CPH plants. The gasifier model used for the analysis is based on and downscaled version of the Viking two-stage gasifier build at DTU-MEK and now located at DTU Risø. The Viking gasifier plant is a 75kWth biomass gasifier using a autothermal (air blown) fixed bed gasifier which produces a clean syngas which can be directly fed into a SOFC, for more information of the gasifier plant turn to [11, 12, 13]. The SOFC is based on theoretical equations with empirical coefficients from an experimental setup. While the Stirling engines parameters is chosen for a fitting a validated feasible engine regards to construction.

METHODOLOGY

The thermodynamic results in this paper were obtained from the simulation tool DNA (Dynamic Network Analysis), see e.g. [14]. The software is a result of an ongoing development process at the thermal energy section at the Mechanical Department of the Technical University of Denmark, which began with a Master's Thesis work [15]. After that the program has been continuously developed to be generally applicable covering unique features and hence supplementing other simulation programs.
The program includes a component library, thermodynamic state models for fluids and standard numerical solvers for differential and algebraic equation systems. The component library contents models ranging from heat exchangers, burners, turbo machinery, dryers, decanters, energy storages, engines, valves, controllers etc. The thermodynamic state models for fluids covers most of the basic fluids and compounds such as ash and tar, used in energy system analyses.
DNA is a component based simulation tool, means that the model is formulated by connection components together with nodes and adding operating conditions to build up a system. Then will the physical model be converted into a set of mathematical equations and solved numerically. The equations will include mass and energy conservation for all components and nodes together will relations for thermodynamic properties of the fluids in the system. The total mass balance and energy balance for the entire system is also included to account for heat loss and heat exchange between different components. In addition, the components include a number of constitutive equations representing their physical properties, e.g., heat transfer coefficients for heat exchangers and isentropic efficiencies for compressors and

turbines. The program is written in FORTRAN and users may also implement additional components and thermodynamic state models to the libraries.
For the thermoeconomy, the general theory is used together with governing component costs equations is used for making of the linear equation system, and solved in Engineering Equation Solver (EES).

Modelling of SOFC stacks

The SOFC model developed in this investigation is based on the planar type developed by DTU-Risø and TOPSØE Fuel Cell (TOFC). The model was calibrated against experimental data in the range of 650°C to 800°C (the operating temperature), as described in [16]. For the sake of clarity, it is shortly described here. The model is assumed to be a zero-dimensional, thus enabling calculation of complicated energy systems. In such modeling one must distinguish between electrochemical modeling, calculation of cell irreversibility (cell voltage efficiency) and the species compositions at outlet. For electrochemical modeling, the operational voltage (U_{cell}) was found to be

$$U_{cell} = U_{Nernst} - \Delta U_{act} - \Delta U_{ohm} - \Delta U_{conc} \quad . \tag{1}$$

Assuming that only hydrogen is electrochemically converted, then the Nernst equation can be written as

$$U_{Nernst} = \frac{-\Delta g_f{}^0}{n_e F} + \frac{RT}{n_e F} \ln\left(\frac{p_{H_2,tot}\sqrt{p_{O_2}}}{p_{H_2O}} \right), \tag{2}$$

$$p_{H2,tot} = p_{H2} + p_{CO} + 4p_{CH4} \tag{3}$$

where Δg_f^0 is the Gibbs free energy (for H_2 reaction) at standard pressure. The water-gas shift reaction is very fast and therefore the assumption of hydrogen as only species to be electrochemically converted is justified, see [17] and [18]. In the above equations p_{H2} and p_{H2O} are the partial pressures for H_2 and H_2O respectively.
The activation polarization can be evaluated from the Butler–Volmer equation, which is isolated from other polarizations to determine the charge transfer coefficients and exchange current density from the experiment by the curve fitting technique see e.g. [19-20].
The ohmic polarization depends on the electrical conductivity of the electrodes as well as the ionic conductivity of the electrolyte see e.g. [21-22]. This was also calibrated against experimental data for a cell with anode thickness, electrolyte thickness and cathode thickness of 600 μm, 50 μm and 10 μm respectively.
The concentration polarization is dominant at high current densities for anode-supported SOFCs, wherein insufficient amounts of reactants are transported to the electrodes and the voltage is then reduced significantly. Again the concentration polarization was calibrated against experimental data by introducing the anode limiting current (see, e.g. [23-24]), in which the anode porosity and tortuosity were also included among other parameters.
The fuel composition at anode outlet was calculated using the Gibbs minimization method as described in [25]. Equilibrium at the anode outlet temperature and pressure was assumed for the following species: H_2, CO, CO_2, H_2O, CH_4 and N_2. Thus the Gibbs minimization method calculates the compositions of these species at outlet by minimizing their Gibbs energy. The equilibrium assumption is fair because the methane content in this study is very low.
To calculate the voltage efficiency of the SOFC cells, the power production from the SOFC (P_{SOFC}) depends on the amount of chemical energy fed to the anode, the reversible efficiency

(η_{rev}), the voltage efficiency (η_v) and the fuel utilization factor (U_F). It is defined in mathematical form as

$$P_{SOFC} = \left(LHV_{H_2}\,\dot{n}_{H_2,in} + LHV_{CO}\,\dot{n}_{CO,in} + LHV_{CH_4}\,\dot{n}_{CH_4,in}\right)\eta_{rev}\,\eta_v\,U_F\ , \tag{4}$$

where U_F was a set value and η_v was defined as

$$\eta_v = \frac{\Delta U_{\text{cell}}}{U_{Nernst}} \tag{5}$$

The reversible efficiency is the maximum possible efficiency defined as the relationship between the maximum electrical energy available (change in Gibbs free energy) and the fuels LHV (lower heating value) as follows, (see e.g. [26])

$$\eta_{rev} = \frac{\left(\Delta\bar{g}_f\right)_{fuel}}{LHV_{fuel}} \tag{6}$$

$$\begin{aligned}\left(\Delta\bar{g}_f\right)_{fuel} = &\left[\left(\bar{g}_f\right)_{H_2O} - \left(\bar{g}_f\right)_{H_2} - \tfrac{1}{2}\left(\bar{g}_f\right)_{O_2}\right]y_{H_2,in}\\ &+\left[\left(\bar{g}_f\right)_{CO_2} - \left(\bar{g}_f\right)_{CO} - \tfrac{1}{2}\left(\bar{g}_f\right)_{O_2}\right]y_{CO,in}\\ &+\left[\left(\bar{g}_f\right)_{CO_2} + 2\left(\bar{g}_f\right)_{H_2O} - \left(\bar{g}_f\right)_{CH_4} - 2\left(\bar{g}_f\right)_{O_2}\right]y_{CH_4,in}\end{aligned} \tag{7}$$

The partial pressures were assumed to be the average between the inlet and outlet as

$$\begin{aligned}\bar{p}_j &= \left(\frac{y_{j,\text{out}} + y_{j,\text{in}}}{2}\right)\bar{p} \qquad j = \{\text{H}_2, \text{CO}, \text{CH}_4, \text{CO}_2, \text{H}_2\text{O}, \text{N}_2\}\\ \bar{p}_{\text{O}_2} &= \left(\frac{y_{\text{O}_2,\text{out}} + y_{\text{O}_2,\text{in}}}{2}\right)\bar{p}_{\text{c}}\end{aligned} \tag{8}$$

In addition, equations for conservation of mass (with molar flows), conservation of energy and conservation of momentum were also included into the model.

Modelling of Stirling engine

The Stirling engine is noted for its quiet operation and the ease with which it can make use of almost any heat source. Stirling engines are referred to as external combustion heat engines, operated based on a regenerative closed power cycle using helium, nitrogen, air or hydrogen as the working fluid. An ideal regenerative Stirling cycle consists of four processes in one cycle. First, the working fluid absorbs the heat from a high temperature reservoir and experiences an isothermal expansion. Second, the hot working fluid flows through a regenerator, and the regenerator absorbs heat from the hot working fluid. Thus, the temperature of the working fluid decreases in an isochoric process. Third, the working fluid rejects heat to a low temperature reservoir and experiences an isothermal compression. Finally, the cold working fluid flows back through the regenerator, and the regenerator rejects heat to the working fluid. The temperature of the working fluid increases in the second isochoric process.

The model of the Stirling engine gives a rater conservative engine related to e.g. efficiency. And used mainly to show the applicability of the technology as a functioning bottoming cycle for usage of a hot exit flow, which in this case is generated by the means of combustion after achieving a rather high temperature even before in the SOFC topping cycle. Further the model parameter inputs are selected so that construction is feasible means no infinite surface areas of

heat exchangers etc. The heat source used in the analysis is the combustion product gasses from the catalytic gas burner, while water used for domestic purposes are used as the sink.
In this study, a pseudo Stirling cycle which has a better agreement to engine performance data is adopted [27]. The power output for the Stirling engine are modeled as

$$P_{Stirling} = \eta_{pcy}\left(Q_{high} - Q_{loss}\right) \tag{9}$$

where Q_{loss} is defined as

$$Q_{loss} = Q_{high}\left(1 - \eta_{mec,stirl}\right) \tag{10}$$

where $\eta_{mec,Stirl}$ is the mechanical efficiency of the Stirling engine and Q_{high} is the amount of heat the Stirling engine absorbs from the hot source. The polytrophic efficiency η_{pcy} is defined accordingly to as [27]

$$\eta_{pcy} = \left[\frac{\left(1 - RV^{1-\gamma}\right) - \zeta\left(RV^{\gamma-1} - 1\right)}{\left(1 - RV^{1-\gamma}\right) + \left(1 - \zeta\right)\left(1 - \varepsilon_{stirl}\right)}\right] \tag{11}$$

where RV, ε_{stirl}, are the reversibility factor for the Stirling engine, the effectiveness of the internal heat exchangers in the engine respectively, whilst the constant γ is 1.667 and ζ defined as the temperature of the cooler gas over the heater gas as

$$\zeta = \left[\frac{T_{cooler,gas} + 273.15}{T_{heater,gas} + 273.15}\right] \tag{12}$$

where $T_{heater\ gas}$ is

$$T_{heater,gas} = T_{heater,wall} - \Delta T_{high} \tag{13}$$

$$T_{cooler,wall} = T_{water,inlet} + 0.66667\left(\Delta T_{water}\right) \tag{14}$$

$$T_{cooler,gas} = T_{cooler,wall} + \Delta T_{low} \tag{15}$$

Modelling of Gasifier

A downscaled version of the two-stage gasifier, Viking is modeled and used for the analysis in this investigation. The Viking gasifier is a 75 kW_{th} gasifier build and developed by the Biomass Gasification Group at the Technical University of Denmark [8]. Wood pellets are used as feedstock, those are firstly dried for removal of surface moisture and pyrolysed in the first reactor, then the pyrolysed products (600°C) is fed into a downdraft fixed bed char gasifier reactor. The produced exhaust gases are used for heating of the reactor for the drying and pyrolysis processes, see Fig. 1. Between pyrolysis and char gasification, partial oxidation of the pyrolysis products provides the heat for the endothermic char gasification reactions. Char is gasified in the fixed bed while H_2O and CO_2 are the gasifying agents in the char gasification reactions. Further the gasifier operates at nearly atmospheric pressure levels.
The gasifier is modeled by implementation of a simple Gibbs reactor, which when reached chemical equilibrium, the Gibbs free energy is at its minimum. Such characteristic is used to calculate the gas composition at a specific temperature and pressure without taking the reaction paths into account [25], and will be briefly explained underneath. The Gibbs free energy of a gas (assumed a mixture of k perfect gases) is shown as

$$\dot{G} = \sum_{i=1}^{k} \dot{n}_i \left[g_i^0 + RT\ln\left(n_i\, p\right)\right] \tag{16}$$

Further, each atomic element in the inlet gas is in balance with the outlet gas composition, which shows that the flow of each atom has to be conserved. For *N* elements, this balance is expressed as

$$\sum_{i=1}^{k} \dot{n}_{i,in}\, \mathbf{A}_{ij} = \sum_{m=1}^{w} \dot{n}_{m,out}\, \mathbf{A}_{mj} \qquad \text{for } j = 1,N \tag{17}$$

where *N* elements corresponds to H_2, O_2, N_2, CO, NO, CO_2, steam, NH_3, H_2S, SO_2, CH_4, C, NO_2, HCN (hydrogen cyanide), COS (carbonyl sulfide), Ar, and Ashes (SiO_2) in the gasifying process. $\mathbf{A}_{mj}$ is the number of atoms of element *j* (H, C, O, N) in each molecule of entering compound *i* (H_2, CH_4, CO, CO_2, H_2O, O_2, N_2, and Ar), whilst $\mathbf{A}_{ij}$ is the number of atoms of element *j* in each molecule of leaving compound *m* (H_2, O_2, N_2, CO, NO, CO_2, steam, NH_3, H_2S, SO_2, CH_4, C, NO_2, HCN (hydrogen cyanide), COS, Ar and Ashes). The minimization of the Gibbs free energy was formulated by introducing a Lagrange multiplier, μ, for each of the N constraints obtained. The expression can be minimized to

$$\phi = \dot{G}_{tot,out} + \sum_{j=1}^{N} \mu_j \left(\sum_{i=1}^{k} \dot{n}_{i,out}\, A_{ij} - \sum_{m=1}^{w} \dot{n}_{m,in}\, A_{mj} \right) \tag{18}$$

Further, by setting the partial derivation of this equation with respect to $\dot{n}_{i,out}$ to zero then the function φ can be minimized as

$$\begin{aligned} &\frac{\partial \phi}{\partial \dot{n}_{i,out}} = \frac{\partial \dot{G}_{tot,out}}{\partial \dot{n}_{i,out}} + \sum_{j=1}^{N} \mu_j \mathbf{A}_{ij} = 0 \qquad \text{for } i = 1,k \\ &\Rightarrow \quad g^{0}_{i,out} + RT \ln\left(n_{i,out} p_{out}\right) + \sum_{j=1}^{N} \mu_j \mathbf{A}_{ij} = 0 \qquad \text{for } i = 1,k \end{aligned} \tag{19}$$

Thus a set of *k* equations are defined for each chemical compound leaving the system.

Modelling of other components

The compressors power consumption are modeled based on the definition of isentropic $\eta_{isentropic}$ and mechanical efficiencies $\eta_{mechanical}$ as

$$\eta_{isentropic} = \left[\frac{W'}{W} = \frac{\Delta h'_0}{\Delta h_0} = \frac{T'_{exit} - T_{in}}{T_{exit} - T_{in}} \right]_{compressor} \tag{20}$$

$$\eta_{mechanical} = \left[\frac{\Delta h_0}{\dot{W}} \right]_{compressor} \tag{21}$$

where the mark ' represents the compression process without isentropic losses.

Heat exchangers are all assumed counter flow and it is assumed that all of the energy is transferred from one to the other side as if heat losses are neglected, both LMTD (Logarithmic Mean Temperature Difference) and ε-NTU (effectiveness-Number of Transferred Unit) methods is used in the calculation of the flows in the heat exchangers depending on the type [28].

For modeling the methanator which is used to increase the content of methane in the fuel, a methanation process is used which is mainly expressed by the exothermic reaction of CO and H_2 are reformed to CH_4 and steam. However some other minor reactions will also occur.

$$CO + 3H_2 \rightarrow CH_4 + H_2O \tag{22}$$

Regarding the catalytic gas burner where unused fuel are reformed in a highly exothermic process are modeled to following the general equation for burning of hydrocarbons in oxygen shown as

$$C_nH_m + (n + \frac{m}{4})O_2 \rightarrow nCO_2 + (\frac{m}{2})H_2O \quad (23)$$

where *n* and *m* denotes the amount present of the hydrocarbon present in the reaction. Further, for all reforming component the analyzing software uses the Gibbs free energy for the different compounds. So that chemical equilibrium is obtained by the minimizing of the Gibbs free energy for the reactions.

The pumps power consumption is obtained by volumetric and pressure states as

$$W_{pump} = \left[\frac{\dot{m} \upsilon_{in} (p_{out} - p_{in})}{\eta} \right]_{pump} . \quad (24)$$

Cost model and cost of components

For the making of the cost model, general theory from [29] is used, for obtaining the costs of each separate stream in the energy system and to determine a cost of the produced electricity and domestic hot water which is considered as a by-product. The system which is modeled together with different components, denoted *k* has different cost associated with it. Cost rates of each component are made as

$$\dot{C}_{P,k} = \dot{C}_{F,k} + \dot{Z}_k^{CI} + \dot{Z}_k^{OM} \quad (25)$$

where $\dot{C}_{P,k}$ is the total cost rate associated by the product of the component, whilst $\dot{C}_{F,k}$ is the cost rate associated with the fuel (inflow) to the component. $\dot{Z}_k^{CI}$ and $\dot{Z}_k^{OM}$ are the cost rates associated with the annual contribution to investment, and operation and maintenance respectively of the component *k* divided by the annual operation time in hours of the system. Thus for finding the cost of the entire system, all components cost balances needs to be taken into consideration.

Regarding the component cost rates, those are found by finding the total capital investment cost (TCI), which is found by defining the purchase cost of each component (PEC). PEC cost equations are shown in Table 1 which obtained from [30] and [32], and are in $.

Table 1. Component investment costs.

Component	Equation
SOFC	$I_{SOFC} = I_{stack,SOFC} + I_{aux,SOFC}$ $I_{stack,SOFC} = (N_{cell} \pi D_{cell} L_{cell})(2.96 T_{cell} - 1907)$ $I_{aux,SOFC} = 0.10 I_{SOFC}$
SOFC Inverter	$I_{SOFC,inverter} = 10^5 \left(\frac{\dot{W}_{el}}{500} \right)^{0.7}$
Compressor	$I_{compressor} = 91562 \left(\frac{\dot{W}_{compressor}}{445} \right)^{0.67}$
Heat exchanger	$I_{hex} = 130 \left(\frac{A_{hex}}{0.093} \right)^{0.78}$
Gas cleaner, methanator and	$I_{PR} = 130 \left(\frac{A_{PR,fin}}{0.093} \right)^{0.78} + 3240 (V_{PR})^{0.4} + 2128 V_{PR}$

catalytic burner	
Pump	$I_{pump} = 442\left(\dot{W}_{pump}\right)^{0.71} 1.41 \times \left[1 + \left(\frac{1-0.8}{1-\eta_{pump}}\right)\right]$
Gasifier	$I_{gasifier} = 1600\left(\dot{m}_{drywood}\right)^{0.67}$

For the SOFC the cylindrical cells with a diameter of 0.005*m* and a length of 0.12*m* are assumed. For the SOFC inverter $\dot{W}_{el}$ is in Watts only, while for the other components, e.g. compressors are in kW.

The cost of Stirling engine is assumed from [1] with the assumption that the total TCI is 2200*$/kW* installed effect. Further, such price represents the present cost, and therefore it is expected to decrease when Stirling engines reach commercialization levels.

Heat exchanger area is calculate by

$$A_{hex} = \left[\frac{\dot{m}\,\Delta h}{k\,\Delta T_{ml}}\right] \tag{26}$$

where the values for *k* are used as 35 W/m^{2}K for gas-gas heat exchangers and 135 W/m^{2}K for gas-liquid heat exchangers. ΔT_{lm} is the logarithmic mean temperature difference of the heat exchangers.

For the fuel reformers (methanator and gas cleaner) the finned area is assumed to be 10 percent of the volume of the fuel reformer. V_{PR} is assumed from the inlet mass flow and the reaction time of the process. Reaction time is assumed from [31] to be 1 second for the gas cleaner and 0.5 seconds for the methanator. The gas burner is assumed to be a catalytic burner and therefore, its equation cost is assumed to be the same as for the fuel reformers.

Gasifier purchase cost is assumed from [32] as due to the small scale of the gasifier and the drywood mass flow is given in *kg/h*.

Purchase cost of splitters, mixers, and valves are neglected due to the sizing and therefore they are considered to be a part of the direct costs related to the investment, e.g. piping, instrumentation and controls.

TCI of PEC for each component *k* are gained form

$$I_k^{tot} = I_k\left(1 + \frac{149}{100}\right)\left(1 + \frac{23}{100}\left(1 + \frac{15}{100}\right)\right) \tag{27}$$

where the relation of direct and indirect costs related to the investment used are shown in Table 2.

Table 2. Estimates of rates for total investment cost

Total capital investment	
Direct costs	Percentage of PEC
(a) Onside costs	
Purchased equipment installation	33%
Piping	35%
Instrumentation and controls	12%
Electrical equipment and materials	13%
(b) Offsite costs	
Civil, structural and architectural work	21%
Service facilities	35%

Indirect costs	
Engineering and supervision	8%
Construction, and contractors profit	15%

From the TCI of each component the two cost rates $\dot{Z}_k^{CI}$ and $\dot{Z}_k^{OM}$ can be derived by taking into account the total investment cost and number of operation hours per year, see e.g. [30].
Then the TCI of component *k* is amortized in *n* years by the annuity factor, by means of the interest factor in which interest rate and rate of inflation are accounted. Construction period, interest rate, and rate of inflation are shown in Table 3. For simplification lifetime of the whole system is assumed 20 years. For the construction period it is assumed that it covers the time from initial planning until final completion and commissioning. Interest rate and inflation rates are assumed from [33] with Denmark as area of reference.

Table 3. Assumed economical parameters for the cost rates

Parameter	Value
Annually operating hours	7500 [h/year]
Interest rate	3 %
Inflation rate	2 %
Equipment lifetime	20 [years]
Construction period	1 [year]
Maintenance factor	1.1

The average price for wood chips are assumed to be approximately 45 DKK/GJ [34], which is then converted into $ per kWh. Transportation costs are not considered, however feedstock are assumed to be derived locally, hence low costs associated.
By adding all component equations, a linear system was built in EES (Engineering Equation Solver) to obtain costs of all streams in the system. Further, for all components a single fuel and product were defined for each component, so that cost balances for all components could be found. No heat loss are considered in the thermodynamic analysis, hence Ėq was neglected. Thus, the system could be solved with adding a number of auxiliary equations based on the assumptions that fuel which flows through a component can be used in a later stage, and therefore the fuel had the same unit costs at inlet and outlet. If the product of a component was composed by two or more streams then the unit cost of those were assumed to be the same. Thus for the heat exchangers and dryer, the hot streams specific energy cost was considered to be equal. Furthermore, for compressors and pumps, the specific energy cost of the inlet ambient air or ambient water are assumed to be zero. For the gas cleaner and gasifier, the disposal costs of sulfur and ash were neglected meaning that the specific energy cost was zero. The splitters outlet streams were assumed to be equal. For SOFC, the assumptions were so that the energy difference of the inlet fuel and the outlet used fuel were the fuel consumption of the SOFC, hence specific energy cost to be equal and secondly, the flue gas was considered as waste, hence specific energy cost was zero. This leads to that the fuel for Stirling bottoming cycles still had costs related to the streams, and if more fuel was left in the fuel (caused by lower fuel utilization factor of SOFC) then such assumption was reasonable and in this way the bottoming cycle was not considered as a full regenerative cycle. For the Stirling engine, two auxiliary equations are needed which are made from the assumption that the outlet stream on the hot side was considered as waste, hence it was zero. Also, the water heater utilizing this was assumed to recover energy from the waste. The second assumption

was that the products from the Stirling components are mechanical power from the engine and therefore the absorbed heat by the heat source leads to

$$c_{P,mec} = \left[\frac{c_{cold,in}E_{cold,in} - c_{cold,out}E_{cold,out}}{E_{cold,in} - E_{cold,out}} \right]. \quad (28)$$

Electricity is considered as the main product of the plant, and heat as secondary product which will be presented as long as electricity is produced. It is thus assumed that internal power consumption is covered by the production hence the internal power cost will be equal to the cost of produced electricity by

$$\text{Price}_{el} = \left[\frac{E_{P,SOFC}c_{P,SOFC} + E_{P,Stirling}c_{P,Stirling}}{E_{P,SOFC} + E_{P,Stirling}} \right]. \quad (29)$$

PLANT CONFIGURATION

The system investigated here is a small scale CHP consisting of an integrated biomass gasification plant with a SOFC system functioning as topping cycle whilst a Stirling engine with a water heater are making up the bottoming cycle, see Fig. 1.

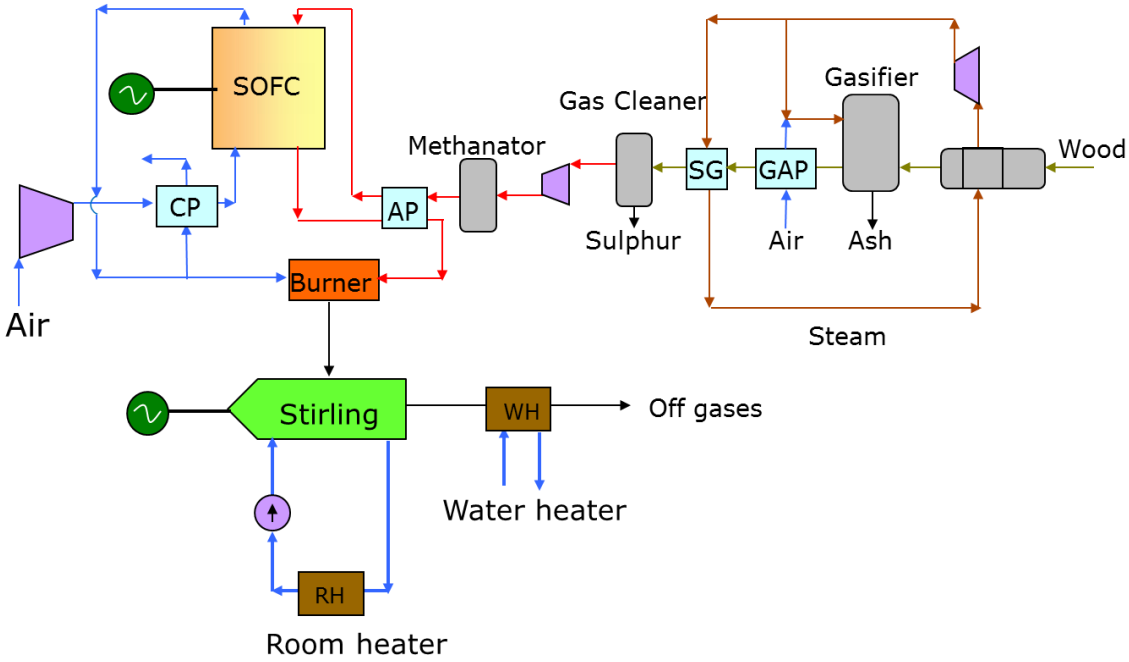

Figure1. System lay-out for the Intergraded Gasification SOFC-Stirling based CHP plant

Wood chips are fed into the system for production of syngas. This is done in a two-step process, wherein the first one is the drying and pyrolysing of the feedstock, and the second process is a fixed bed gasifier, were the pyrolysed feedstock is going to be gasified by steam and air as gasification agents. Air is preheated in a heat exchanger (GAP) before sending to the gasifier. Fuel is dried using a steam loop in which a steam generator (SG) provides the needed steam for drying the fuel. Even though reported in [13] that the produced syngas is clean enough to be fed directly into the SOFC without additional fuel processing, a gas cleaner is introduced for removal of small containments presented in the syngas, mainly sulfur. The gas cleaner is assumed working at a temperature of 250°C.

For the topping SOFC cycle, the ambient air at 15°C is compressed to the working pressure of the SOFC (normal pressure) before being heated up in the cathode air preheater (CP) to cathode inlet temperature of 600°C. The cathode preheater uses some of the SOFC off-air for

the heating. The off-air is split in two streams; one entering the CP and the other one entering the catalytic burner (CB). For the anode side, firstly the cleaned syngas is pumped to compensate the pressure drop along its way. Then the syngas is reformed exothermically in a methanator, wherein CH4 content in the gas is increased from a molar fraction of about 0.01 to nearly 0.05. This is on extent of the molar fraction of H2, CO, and steam, while N2 and CO2 also have also increased the share of the molar fraction of the gas. This will not inflict the SOFCs electrical production in any particular way, however due to the fact that the reformation is highly exothermic less heat is needed to be extracted from the SOFC off-fuel to heat up the incoming fuel to the SOFC fuel inlet temperature of 650°C in the anode preheater (AP). This will eventually lead so that the Stirling engine will get a larger amount of heat to be used, which is caused by the fact that the fuel will have a higher temperature when entering the CB, and therefore the combustion processes takes place at higher temperature. The CB is implemented since all the fuel is not reacted in the SOFC stacks due to fuel utilization. The entering temperatures are essential requirements for proper functioning of SOFC stacks, not only to initiate the chemical reactions but also for avoiding cell thermal fractures.
Secondly, a larger portion of CH4 in SOFC causes endothermic internal reforming, which leads to less air will be used to cooling purpose to maintain the SOFC operating temperature at 780°C. It means that the workload of the cathode compressor/air blower will decrease.
For the bottoming cycle, a Stirling engine is implemented. The Stirling engine utilizes the combustion products leaving the CB as the heat source. For the heat sink, water is used with an incoming temperature of 20°C and an exit temperature of 60°C so that it can be used as e.g. hot water for room heating, not only at a temperature that is enough for addressing problems related to bacteria's e.g. Legionella [35], but also sufficient high temperature for heating (and/or domestic) purposes. The remaining heat after the Stirling engine is used for domestic water heating. Water is constrained in the same manner as the heat sink and the combustion products leaves the system into the environments at about 95°C, high enough to avoid corrosion problems.

RESULTS AND DISCUSSIONS

The main operating parameters for the plant are presented in Table 4. Ambient conditions are assumed to be 1bar and 15°C. The presented values are the final ones used after the optimization.

Table 4. System operating input parameters

Parameter	Value
Wood chips temperature	15 °C
Dry wood temperature	150 °C
Gasifier temperature	800 °C
Gasifier pressure drop	0.005 bar
Gasifier carbon conversion factor	1
Gasifier non-equilibrium methane	0.01
Steam blower isentropic efficiency	0.8
Steam blower mechanical efficiency	0.98
Steam temperature in steam loop	150 °C
Wood gas blower isentropic efficiency	0.7
Wood gas blower mechanical efficiency	0.95
Gas cleaner pressure drop	0.0049 bar
Cathode compressor air intake temperature	25°C
Compressor isentropic efficiency	0.7

Compressor mechanical efficiency	0.95
SOFC operating temperature	780°C
Anode inlet temperature	650°C
Cathode inlet temperature	600°C
Pressure drop anode side	0.02 bar
Pressure drop cathode side	0.055 bar
SOFC fuel utilization rate	0.675
Number of cells in stack	74
Number of stacks	160
Heat exchangers pressure drop	0.01 bar
Pinch temperature CP	20 °C
Burner ratio inlet outlet pressure	0.97
Stirling engine heater wall temperature	600 °C
Stirling engine ΔT_{high}	125 °C
Stirling engine ΔT_{low}	60 °C
RV Loss factor regenerator Stirling engine	1.44
Heat exchanger efficiency Stirling engine	0.98
Stirling engine mechanical efficiency	0.8
Water pump efficiency	0.95
Inlet water temperature water heater	20 °C
Outlet water temperature water heater	60 °C
Outlet combustion products temperature water heater	95 °C

For achieving the 120kW output of electrical energy, the gasifier needs an input of about 89.4kg/h, which leads to a syngas production of about 176.4kg/h. This means that such amount of biomass shall be provided to the unit, either by available biomass from agriculture or from a cultivation area. The syngas molar fraction is presented in Table 5.

Table 5. Syngas molar fraction composition

Compound	Molar fraction
Hydrogen	0.219
Nitrogen	0.309
Carbon monoxide	0.085
Carbon dioxide	0.185
Water (g)	0.146
Methane	0.048
Argon	0.003

Since ambient air is used as one of the gasifying agents, a large portion of unusable N2 is present in the syngas. AS seen, some steam is also presented in the syngas because such small scale gasifier cannot completely dry up the produced gas. This eases application of a methanator prior to SOFC without using anode recirculation or external steam supplement. On the other, this leads to a larger mass flows which is also beneficial for Stirling engine operation. For SOFC, however, large amount of N2 and steam causes concentration polarization at rather early stage. The SOFC has a power output of 98.8kW, while Stirling engine provides 26.9kW of power. Internal power consumption is 5.8kW, which is mainly due to cathode air compressor. The high power consumption for cathode air compressor is

because this compressor also provides cooling effect needed to maintain the SOFC temperature at the desired level. The reaction inside the SOFC is highly endothermic and therefore it needs relatively large flow of air for cooling of the cells.
The thermal efficiency of the topping SOFC cycle is 0.329 LHV, which is somewhat low range for a SOFC system. However, the entire plant has a thermal efficiency of 0.424 LHV, which is a decent value for such a small scale system. The implementation of the bottoming Stirling engine gives a remarkable increase in plant efficiency of 28.9 percent, see Table6.

Table 6. Plant output for the initial operating parameters

Parameter	System output
Feedstock consumption	89.4*kg/h*
Produced amount of syngas	176.4*kg/h*
Power output SOFC	98.8kW
Power output Stirling engine	26.9kW
Total power consumption	5.8kW
Thermal efficiency SOFC cycle	0.329
Thermal efficiency of plant	0.424
Percentage increase when adding Stirling cycle	28.9%
Component	Produced Heat [kW]
Stirling engine	53.5
Water heater	73.83
Total hot water production	127.33

It is found that the water heater produces nearly two third of the total heat produced. The two heaters (water heater and room heater) together produce 127.33kW.
It is also assumed that the plants internal electrical consumption is covered by its production, meaning that the 120kW production of electricity is the net production

$$P_{net} = P_{SOFC} + P_{Stirling} - \Sigma_n P_{el,n,consumed} \quad (30)$$

where $P_{el,n,consumed}$ is the consumption of power from the n'th component. The thermal efficiency of the plant is calculated by the net power production SOFC and the Stirling engine compared to fuel input as

$$\eta_{th,plant} = \left[\frac{P_{net}}{\dot{m}_{fuel} \times LHV_{fuel}} \right] \quad (31)$$

Thermodynamic investigation

The most important parameters to be investigated are woodchips mass flow, number of SOFC stacks and SOFC cell utilization factor. The woodchips mass flow indicates the cultivation area to be allocated for providing the needed mass flow of the fuel. Number of SOFC stacks is directly related to the SOFC purchased cost and thereby investment cost while utilization factor affects the amount of off-fuel (rest fuel after the SOFC stacks) which would be available for the bottoming cycle (Stirling engine in this case). The lower utilization factor means that more fuel will be available for the Stirling engine and therefore the engine will produce more power. In other words, the utilization factor affects the cooperation between the two cycles namely SOFC plant and Stirling engine.
Following the discussions above the first parameters to be investigated was the woodchips mass flow. In order to study the system performance with different woodchips mass flow, the initial analysis was performed on a system using 100 and 150 SOFC stacks with 74 cells for

each stack. Fuel utilization for SOFC cells was assumed to be 0.8. The final utilization factor will decided later on. Plant efficiency and net power production as function of woodchips mass flow are shown in Fig. 2.

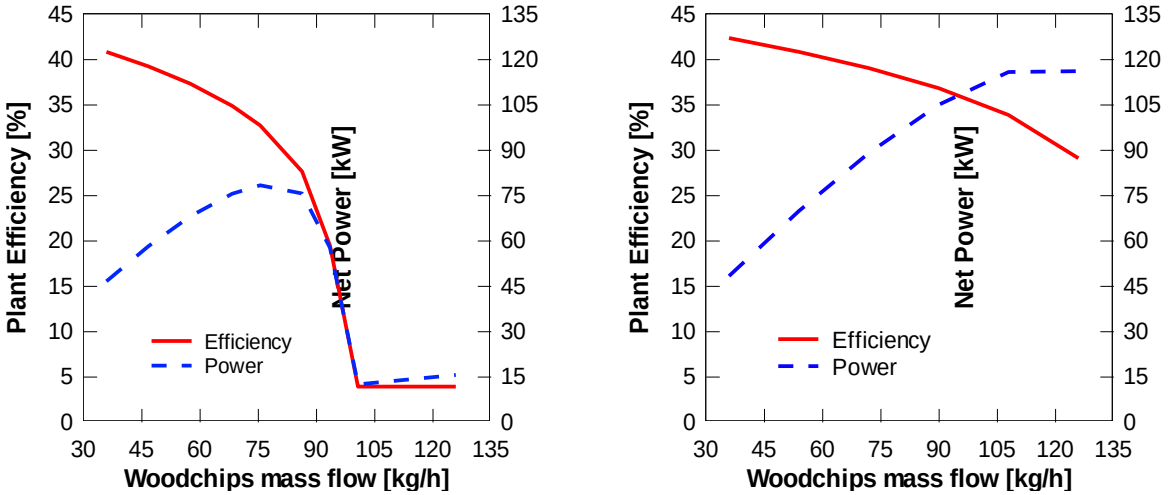

Figure 2. Plant thermal efficiency and net power production as function of woodchips mass, a) 100 stacks and b) 150 stacks.

As shown the thermal efficiency of the system tends to drop as the mass flow in the system increases, at a certain level of fuel mass flow it tends to drop drastically. For the case with 100 stacks, the power increases as the woodchips mass flow increases to reach a maximum and then tends to decrease as the fuel mass flow is further increased. Such a behavior is also true for the case with 150 stacks but with much higher woodchips mass flow instead. Assuming other values for SOFC utilization factor than 0.8 then the results will be slightly changed but the overall conclusions remains the same.

Another important parameter to be studied is the SOFC utilization factor. To study this parameter the woodchips mass flow is fixed to produce a net power of 120 kW at utilization factor of about 0.7. Figure 3 shows the variation of plant efficiency and net power production when SOFC utilization factor is changed. The results are shown for two different numbers of stacks (100 stacks respective 150 stacks) to study the plant performance.

Several interesting points can be concluded from this figure. There exist a utilization factor for which the plant efficiency is maximum; 0.625 for 100 stacks and 0.65 for 150 stacks. Such maxima point is unique for a certain number of stacks which must be found out whenever the number of stacks is decided from economic analysis. Another issue to be mentioned is that the net power production as well as plant efficiency decreases sharply after a certain utilization factor. This point is found out to be about 0.8 for 100 stacks and 0.83 for 150 stacks. At this point the concentration losses in the SOFC cells dominate, and as a result the cell voltage decreases significantly. Obviously this point will be shifted to the right when number of stacks is increased. Increasing number of stacks decreases the fuel amount for each stack when total fuel mass flow remains constant.

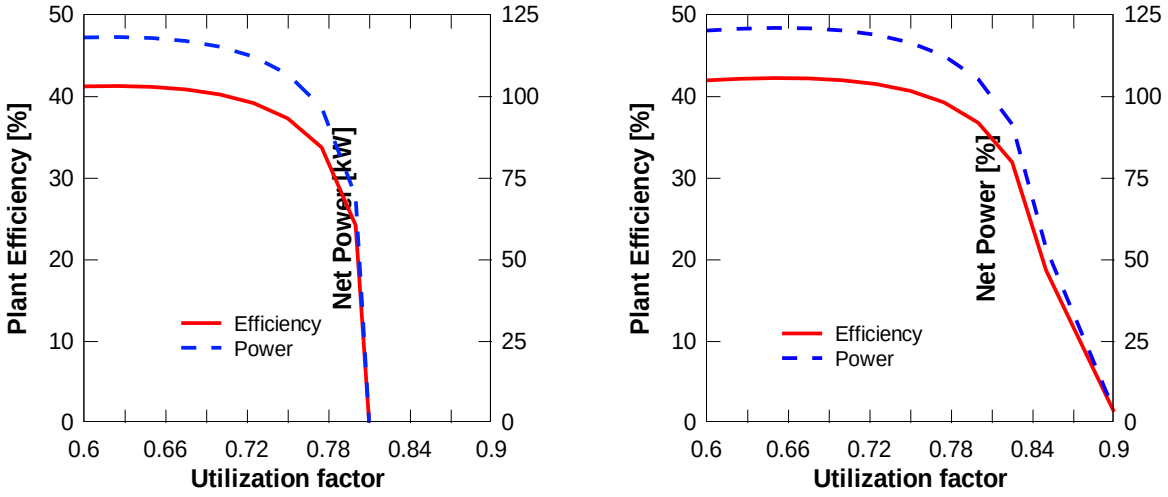

Figure 3. Plant thermal efficiency and net power production as function of utilization factor when woodchips mass is fixed, a) 100 stacks and b) 150 stacks.

As mentioned above the number of stacks is also an important issue to be studied. For this reason several calculations were performed and the results are illustrated in Fig. 4. For distinguish purposes two utilization factors are selected; 0.8 which is a rather high value and 0.65 which was the optimum value when 150 stacks were used. Again the fuel mass flow is fixed for these cases. For the case with 0.8 utilization factor, increasing stack number from 100 to about 120 numbers increases plant efficiency and power sharply and further increase of stack numbers increases plant performance significantly. Eventually, the amount of fuel per stack is too large and ionic concentration has reached its limit. Increasing stack numbers distributes the fixed fuel to more stacks and releases the concentration below its limit.

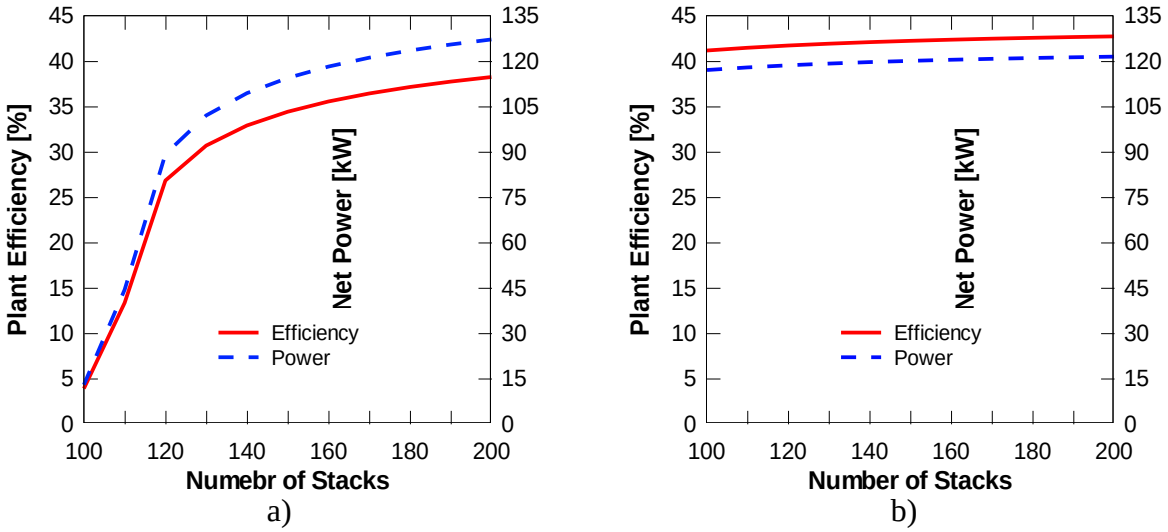

Figure 4. Plant thermal efficiency and net power production as function of number of stacks when woodchips mass is fixed, a) utilization factor = 0.8 and b) utilization factor = 0.65.

For the case with 0.65 utilization factor, increasing stack numbers increases plant efficiency and power slightly. The problem of ionic concentration does not exist for such relatively low utilization factor. Another conclusion from these results is that the plant efficiency for the case with 0.65 utilization factor is higher than the case with 0.8. However, the power produced with 0.8 utilization factor could be more than the power produced with 0.65 utilization factor if the number of stacks are high enough (more than about 160 stacks).

Number of stacks is directly associated with plant investment cost and therefore a limit must be chosen to avoid high investment cost as well as price of produced electricity. The higher the number SOFC stack is the higher associated investment cost would be. By closer inspection of Fig. 4, choosing 160 SOFC results in rather high plant efficiency compared to 120 stacks. On the other hand, the investment cost of 160 SOFC stacks is significantly lower than 200 stacks. Preliminary test results showed that choosing 160 will be a reasonable value from plant efficiency as well as investment cost. For this reason, 160 stacks are chosen from now on for analyzing the cost, even though other values could be selected.

Thermoeconomical investigation

Based on the results from the thermodynamic analysis and then combined with the cost equations of each component along with economic parameters, the operation cost per hour [$/hour] was obtained, see Table 7. The operation cost is denoted Z^{tot}, which is the component investment cost over its lifetime. The operation and maintenance cost are denoted Z^{CI} respective Z^{OM}.

Table 7. System and component cost rates [$/hour]

Component	Z^{CI} [$/hour]	Z^{OM} [$/hour]	Z^{tot} [$/hour]
SOFC	0.834445	0.917889	1.752
Inverter	0.007102	0.007812	0.015
AP	0.030144	0.033158	0.063
Methanator	0.035623	0.039185	0.074
Syngas compressor	0.055377	0.060914	0.116
Gas Cleaner	0.057162	0.062878	0.120
CP	0.579426	0.637368	1.217
Cathode compressor	0.103230	0.113553	0.217
Catalytic gas burner	0.103073	0.113380	0.216
Stirling engine	0.396511	0.436163	0.833
Water pump	0.003295	0.003625	0.007
Water heater	0.043093	0.047402	0.090
Gasifier	0.714470	0.785917	1.500
GAP	0.062926	0.069219	0.132
Steam generator	0.057336	0.063069	0.120
Steam loop blower	0.030753	0.033828	0.065
Total operating cost	2.949469	3.244416	6.194

As the table shows, the largest cost is associated with the SOFC of 1.752 *$/hour*, here with 160 stacks and 74 cells in each stack, followed by the gasifier 1.5 *$/hour*, then CP (cathode air preheater) 1.217 *$/hour* which is a relatively a large heat exchanger, and the Stirling engine 0.833 *$/hour*. For the other components the costs are relatively low. The entire plant's operating cost is found to be 9.447 *$/hour*, with the current inputs and assumptions.
Systems sensitivity to the fuel price is illustrated in Fig. 5, for which the system costs shown in Table 7 are used. As seen increasing the fuel price with 0.02 *$/kWh* increases the produced electricity price by approximately 0.05 *$/kWh*. For the system with the current price of wood chips described in the cost model section, a production price of 0.1215 *$/kWh* is found. The price of produced domestic hot water (the price of DHW) was found to be 0.0219 *$/kWh*. Such low cost is caused by the assumption that the cost of DHW is the cost rate of the water heater and the energy difference of the "in" and "outflow" of the WH and the Stirling engine.

Hence DHW is considered as a byproduct of the plant because electricity is assumed to be the main product, and therefore the cost of the DHW will be how to utilize that heat.

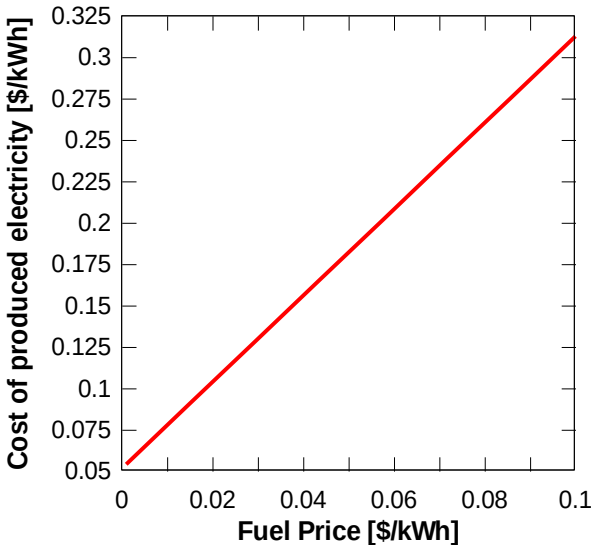

Figure 5. Cost of produced electricity over the Fuel price [$/kWh]

There are several options for reducing the cost of the system. As Table 7 suggests, SOFC is the far most contributing component to the total operating cost, and since the number of stacks is a major part in the cost (see Eq. 37) and therefore reducing number of stack will reduce the component investment cost significantly. However as shown in Fig. 3, reducing the number of stacks will reduce the thermal efficiency of the plant, and since the fuel cost is relatively low then the produced electricity cost will be reduced with a decreasing number of stacks, see Fig. 6.

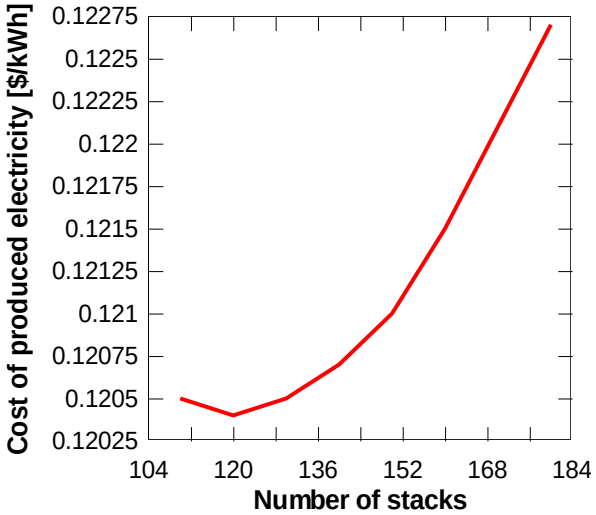

Figure 6. Cost of produced electricity over the number of stacks in the SOFC

As illustrated in Fig. 6, the produced electriccity cost is minimized when number of of SOFC stacks are about 120. This suggests that with the current pricing, it would be more profitable to reduce the number of stacks to about 120 stacks and thereby increasing the amount of feedstock to the gasifier, which in turn decreases plant thermal efficiency but on the other hand the cost of electricity will also be decreases. Thus the number of SOFC stakcs can be found by thermoeconomical optimization. Decreasing numebr of stacks to 120 resulsts in different plant performance which is shown in Table 8.

Table 8. Plant performance by thermoeconomical optimization

Parameter	Value
Produced amount of syngas	180.05 *kg/h*
Fuel consumption	91.33 *kg/h*
Power output SOFC	98.48 *kW*
Power output Stirling engine	27.62 *kW*
Total internal power consumption	6.10 *kW*
Thermal efficiency SOFC cycle	0.3195
Thermal efficiency of the plant	0.4149
Increase when adding bottoming cycle	29.88 *%*
Produced heat	130.52 *kW*
Cost of electricity	0.1204 *$/kWh*
Cost of DHW	0.0214 *$/kWh*
Total TCI over installed capacity	3432.97 *$/kW*

The fuel consumption of 91.33 kg/h of wood is needed to be fed to the gasifier for achieving a net power production of 120 kW. This amount of feedstock to the gasifier will lead to a syngas production of 180.05 kg/h, which means that an air intake to the gasifier is nearly equal to that of wood, for the gasification processes. After methanation of the syngas (for slightly increasing the methane content), the power production of the SOFC plant will be about 98.48 kW. As explained earlier, the methanator increases the amount of methane in the fuel which in turn results in endothermic internal reforming. This will lead to that a smaller amount of air in the cathode side is needed to cool the SOFC to maintain the SOFC operation temperature. Thus the power consumption of the compressor will also be reduced. The total internal power consumption will be about 6.10 kW. The power production from the Stirling engine is about 27.62 kW, leading to plant thermal efficiency of 0.41 (LHV based). The integrated gasification and SOFC topping cycle will have a thermal efficiency of 0.32 (LHV based). Thus applying the Stirling engine as bottoming cycle, increases plant thermal efficiency by nearly 28 percent, which is significant. This is due to the fact that the integrated gasification and SOFC plant has a low thermal efficiency and therefore more energy will be available for the bottoming cycle. A thermal efficiency of 41% sounds to be somewhat low, but for an integrated gasification plant producing only 120 kW is in fact high enough. Note that an integrated gasification combined cycle has an efficiency of about 40% at about 500 MW power output. Note also that SOFC fuel utilization is relatively low, 0.675 as explained earlier. Further130.52 kW of district heat water s produced as a byproduct.

The cost of produced electricity is 0.1204 $/kWh, and the cost of produced DHW is 0.0214 $/kWh. These prices will be changed if the assumptions given above are changed. However, the results obtained here give a relatively good overview on the cost situation.

The obtained costs are a result of low fuel costs and high component and installation costs with respect to the plant size. As stated in energy.eu [36], that electricity price for a household with a consumption of 7500kWh/year (±30%) is 0.2562€/kWh in Denmark, and for the industry with a consumption of 2GWh/year (±50%) the price is 0.0982€/kWh. The obtained results with today's exchange rate from € to $ leads to an electricity price that are within the border of what to be expected when buying it from the grid, hence the system most likely to be competitive for installation in places such as a hotel, malls, etc. It means that the system might be cost effective when SOFC and Stirling engine enter the commercialization phase and their price will be close to what it is predicted here. Regarding DHW here it is considered

to be a byproduct and the cost is obtained as 0.0214 $/kWh, which is much lower than the price of district heating networks as 0.1143$/kWh provided by København Energi 2012 [37]. Thus, for in-house usage the electricity is produced at cost level that is nearly competitive when fuel prices are held at the assumed level. However, for selling the electricity to the grid, the production cost is considered to be high. Comparing to other renewable energy sources at similar size, conventional biomass gasifiers at 20-50000kW sizes produces energy with approximately 0.13 $/kWh, while small scale wind turbines produces energy at even higher rates [38].
Here, the total TCI for installed capacity is 3432.97 $/kW, which is in the higher range when compared to other renewable energy systems.

CONCLUSIONS

A small scale integrated gasification SOFC-Stirling CHP plant with a net capacity of 120kW is presented. Both thermodynamic and thermoeconomic investigations are analyzed. A rather modest plant thermal efficiency is found to be 0.41 after thermoeconomic optimization. This was also partly because the parameter inputs for the different components have been chosen from a conservative point of view, and partly because the produced syngas have a large fraction of non-usable compounds which in turn resulted in lower utilization factor for SOFC stacks.
The thermoeconomical analyses showed that by reducing the number of stacks from 160 stacks with 74 cells to 120 stacks, the cost of produced electricity will be decreased in expense of lower plant thermal efficiency. An electricity production price of 0.1204 $/kWh is found with a DWH production cost of 0.0214 $/kWh, based on assumption of component cost equations for future pricing of SOFC and Stirling engine when emerged into commercialization phase. These prices are competitive in the Danish market for in-house usage but slightly higher if the electricity is sold to the grid.
Neglecting different disposal costs, the plant cost is estimated to 3433 $/kW which is competitive when compared to the other types of environmentally friendly energy systems at similar size.

NOMENCLATURE

A_{hex}	Heat exchanger area, m^2
$\mathbf{A}_{i,j}$	Matrix
$\dot{C}_P$	Product cost rate, $/kWh
$\dot{C}_F$	Fuel cost rate, $/kWh
c_p	specific energy cost, $/kW
D_{cell}	Cell diameter, m
E	Energy, kJ/kg
F	Faradays constant, C/mol
f	Annuity factor
f_η	Efficiency correction factor
k	Thermal conductivity, W/m^2K
g^0	Standard Gibbs free energy, J/mol
g_f	Gibbs free energy, J/mol
h	Enthalpy, J/kg
h_f	Enthalpy of formation, J/mol
I_{comp}	Purchase cost of component k
L_{cell}	Cell length, m

$\dot{m}$	Mass flow rate, kg/s
$\dot{n}_{H2}$	Molar reaction rate of H_2, mol/s
n_e	Number of electron
P	Power, W
p	Pressure, bar
p_{H2}	Partial pressures for H_2 , bar
p_{H2O}	Partial pressures for H_2O, bar
Q	heat, J/s
q_i	Interest rate
T	Operating temperature, K
t	Thickness, m
R	Universal gas constant, J/K mol
RV	Reversibility factor
U_F	Fuel utilization factor
U	Voltage, V
V	Volume, m^3
V_{an}	Anode porosity
W	Work, W
y	Molar fraction
Z^{CI}	Annual contribution to investment, $/kWh
Z^{OM}	Annual contribution to operation and maintenance, $/kWh

Greek symbols

Δ	Change/difference
ΔT_{ml}	Logarithmic mean temperature difference, K
ε	Effectiveness factor
η	Efficiency
η_{pcy}	Polytrophic efficiency
υ	specific volume, m^3/kg

Subscript

act	Activation polarization
an	Anode
aux	Auxiliary
ca	Cathode
conc	Concentration polarization
el	Electricity
FC	Fuel cell
mec	Mechanical
Nernst	Nernst ideal reversible voltage
ohm	Ohmic polarization
ref	Reference
rev	reversible
th	Thermal
v	Voltage

Abbreviations

AP	Anode pre-heater
CHP	Combined Heat and Power

CP Cathode air pre-heater
DHW Domestic Hot Water
DNA Dynamic Network Analysis
EES Engineering Equation Solver
GAP Gasifier air pre-heater
CB Catalytic burner
GT Gas turbine
LHV Lower heating value
SG Steam generator
PEC Component purchase cost
SOFC Solid oxide fuel cell
TCI Total investment cost
WH Water heater

REFERENCES

1. Sanchez D., Chacartegui R., Torres M., Sanchez T., Stirling based fuel cell hybrid systems: an alternative for molten carbonate fuel cells, *J Power Sources*, Vol. 192: pp. 84-93, 2008.
2. Rokni M. Plant Characteristics of a Multi-Fuel SOFC-Stirling Hybrid Configuration. 5th International Conference on Sustainable Energy and Environmental Protection – SEEP2012, 5 – 8 June, Dublin City University, Dublin, Ireland, ISBN: 978-1-873769-11-9, 2012; 269-274.
3. Calise F., Dentice d'Accadia M., Palombo A., Vanoli L., Simulation and exergy analysis of a hybrid solid oxide fuel cell (SOFC)–Gas turbine system, *J Energy*, Vol. 31, pp.3278–99, 2006.
4. EG&G and G Technical Services Inc, *Fuel Cell Handbook*, edition 7, U.S. Departement of Energy, Office of Fossil Energy, National Energy Technology Laboratory, 2004.
5. Riensche E., Achenbach E., Froning D., Haines M.R., Heidug W.K., Lokurlu A. and Adrian S., Clean combined-cycle SOFC power plant–cell modeling and process analysis. *J Power Sources*, Vol. 86, No. 1-2, pp. 404-410, 2000.
6. Pålsson J., Selimovic A., Sjunnesson L., Combined solid oxide fuel cell and gas turbine systems for efficient power and heat generation, *J Power Sources*, Vol. 86, No. 1, pp. 442-448, 2000.
7. Rokni M., Plant characteristics of an integrated solid oxide fuel cell and a steam cycle. *J Energy*, Vol. 35, pp. 4691–99, 2010.
8. Proell T, Aichering C, Rauch R, Hofbauer H. Coupling of biomass steam gasification and SOFC-gas turbine hybrid system for highly efficient electricity generation. *ASME turbo Expo Proceeding*, GT2004-53900, pp. 103-112, 2004.
9. Bang-Møller C., Rokni M., Thermodynamic Preformance Study on Biomass Gasification, Solid Oxide Fuel Cell and Micro Gas Turbine Hybrid Systems. *J Energy Conversion and Management*, Vol. 51, pp. 2330-2339, 2010.
10. Rokni M., Thermodynamic investigation of an integrated gasification plant with solid oxide fuel cell and steam cycles, *J Green*, Vol. 2: pp. 71–86, 2012.
11. Henriksen U, Ahrenfeldt J, Jensen TK, Gøbel B, Bentzen JD, Hindsgaul C, Sørensen LH. The design, construction and operation of a 75 kW two-stage gasifier, *J Energy*, Vol. 31 No. 10-11, pp. 1542-1553, 2006
12. Ahrenfeldt J., Henriksen U., Jensen T.K., Gøbel B., Wiese L., Kather A., Egsgaard H., Validation of a continuous combined heat and power (CHP) operation of a two-stage boimass gasifier, *J Energy and Fuels*, Vol. 20, No. 6, pp. 2672-2680, 2006.

13. Hofmann P.H., Schweiger A., Fryda L., Panopoulos K., Hohenwarter U., Bentzen J., Ouweltjes J.P., Ahrenfeldt J., Henriksen U., Kakaras E., High temperature electrolyte supported Ni-GDC/YSZ/LSM SOFC operation on two stage Viking gasifier product gas. *J Power Sources*, Vol. 173, No. 1, pp. 357-366, 2007.
14. Elmegaard B., Houbak N., DNA – A general energy system simulation tool, *proceeding of SIMS*, Trondheim, Norway; 2005.
15. Perstrup C., Analysis of power plant installation based on network theory (in Danish), *M.Sc. thesis*, Technical University of Denmark, Laboratory of Energetics, Denmark; 1989.
16. Petersen T.F., Houbak N., Elmegaard B., A zero-dimensional model of a 2nd generation planar SOFC with calibrated parameters. *Int. J. Thermodynamic*, Vol. 9, No. 4, pp. 161–169, 2006.
17. Holtappels P., DeHaart L.G.J., Stimming U., Vinke I.C. and Mogensen M., Reaction of CO/CO2 gas mixtures on Ni-YSZ cermet electrode. *J Applied Electrochemistry*, Vol. 29: pp. 561–568, 1999.
18. Matsuzaki Y. and Yasuda I., Electrochemical oxidation of H2 and CO in a H2-H2O-CO-CO2 system at the interface of a Ni-YSZ cermet electrode and YSZ electrolyte. *J Electrochemistry Society*, Vol. 147, No. 5, pp. 1630–35, 2000.
19. Keegan K.M., Khaleel M., Chick L.A., Recknagle K., Simner S.P. and Diebler J., Analysis of a planar solid oxide fuel cell based automotive auxiliary power unit. *SAE technical paper series* No. 2002-01-0413, 2002.
20. Prentice G. *Electrochemical Engineering Principles*. Prentice Hall International, Houston, USA, 1991.
21. Achenbach E. Three-dimensional and time-dependent simulation of a planar solid oxide fuel cell stack. *J Power Sources*, Vol. 49, No. 1–3, pp. 333–348, 1994.
22. Zhu H. and Kee R.J., A general mathematical model for analyzing the performance of fuel-cell membrane-electrode assemblies. *J Power Sources*, Vol. 117, pp. 61-74, 2003.
23. Costamagna P., Selimovic A., Del Borghi M. and Agnew G., Electrochemical model of the integrated planar solid oxide fuel cell (IP-SOFC), *J Chemical Engineering*, Vol. 102, No. 1, pp. 61–69, 2004.
24. Kim J.W. and Virkar A.V., The effect of anode thickness on the performance of anode-supported solid oxide fuel cell. In: Proceedings of the sixth international symposium on SOFCs, (SOFC-VI), PV99-19. *The Electrochemical Society*, pp. 830–839, 1999.
25. Smith J.M., Van Ness H.C. and Abbott M.M., *Introduction to chemical engineering thermodynamics*. 7th ed. Boston: McGraw-Hill; 2005.
26. Winnick, J. *Chemical engineering thermodynamics*, John Wiley &Sons, New Yourk, 1997.
27. Reader GT. The Pseudo Stirling Cycle – A suitable performance criterion, Proceeding of the 13th intersociety energy conversion engineering conference. Vol. 3, pp. 1763–770, San Diego, California, August 20–25, 1979.
28. Incropera F.P., DeWitt D.P., Bergman T.L. and Lavine A.S., *Introduction to Heat Transfer*, 5th ed, Wiley 2006, ISBN 978-0471457275.
29. Bejan A., Tsatsaronis G., Moran M., *Thermal design and optimization*. New York: John wiley and Sons Inc.; 1996.
30. Arsalis A., Spakovsky M., Calise F., Thermoeconomic modeling and parameter study of hybrid solid oxide fuel cell-gas turbine-steam turbine power plants ranging from 1.5 MWe to 10MWe, *J Fuel Cell Science and Technology*, Vol. 6, pp. 011015, 2009.
31. Gary J.H., Handwerk G.E., Kaiser M.J., *Petroleum refining, technology and economics*. 5th edition, CRC press, 2007, ISBN: 0849370388.
32. Kempegowda R.S., Tran K.Q., Skreiberg Ø., Economic analysis of combined cycle biomass gasification fuelled SOFC systems. *International Conference on Future Environment and Energy (ICFEE 2011)*, pp. 134-141, 2011.

33.*Trading Economics August 2012*. (Available online) from http://www.tradingeconomics.com/denmark
34.*Ea Energy Analysis*, Analysis of the market for bio energy, locally and internationally, Series: NEI-DK-5426, sys.no.: 000492186, 2010.
35.Institute of Plumbing & Heating Engineering, *Safe hot water temperature*, July 2012. (Available online): http://www.chipe.org.uk/Global/databyte/safe%hot%water.pdf.
36.*European Union*, August 2012. (Available online): http://www.energy.eu.
37.Københavns Energi, August 2012. (Available online): http://www.ke.dk/portal/page/portal/Erhverv/Varme/prisen_paa_fjernvarme_2012?page=916.
38.*Renewables 2011*. Global status report. REN 21, Renewable energy policy for the 21st Century, Paris, 2011.